Supplementary material

Assessing the ammonia characteristics over a high-altitude mountain site in Shanxi province, China: a comparison with the observations in the North China Plain

Weiwei Pu et al.

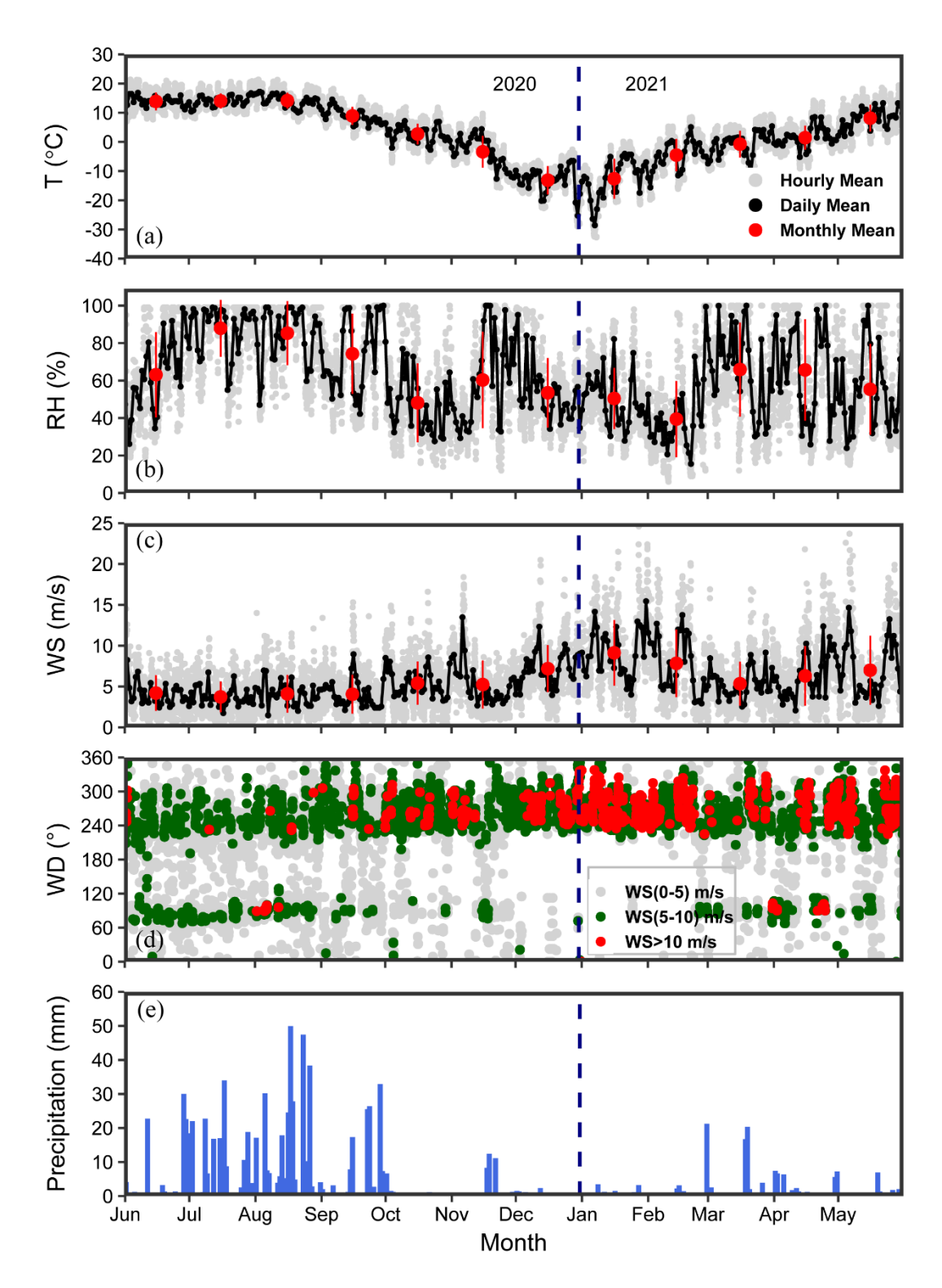


Fig. S1. Observed meteorological variables from the site: T (a), RH (b), WS (c), WD (d), and daily precipitation (e).

Table S1 Statistics of NH₃ at WTS for all four seasons.

Period	Mean	SD	Minimum	P25	Medium	P75	Maximum
All	9.0	6.7	0.1	3.5	7.7	12.7	52.7
Spring	8.9	6.3	2.7	5.0	7.5	10.6	52.7
Summer	15.9	5.4	6.1	11.7	15.4	19.6	35.6
Autumn	8.8	4.2	2.2	5.7	8.1	11.4	22.4
Winter	2.1	1.2	0.14	1.5	2.0	2.4	8.2

Table S2 Comparison of NH₃ concentrations at different high-altitude sites.

		Tuble 32 Comparison of 1413 Concentrations at affective linguisticate sites.						
Site Name	Land use types	Altitude (m) and Location	Observation Period	Sampler type	NH ₃ (ppb)	Reference		
WTM, China	Mountain and forest	2208 (38.95°N, 113.52°E)	Jun 2020 – May 2021	online	9.0 ± 6.7	This study		
Waliguan, China	Grassland	3372 (36.30°N, 100.90°E)	Sep 2015 – Aug 2016	offline	3.0	Pan et al. (2018)		
Ailaoshan, China	Mountain and forest	2483 (24.30°N, 101.00°E)	Sep 2015 – Aug 2016	offline	2.0	Pan et al. (2018)		
Gongashan, China	Mountain and forest	2977 (29.60°N, 102.00°E)	Sep 2015 – Aug 2016	offline	2.6	Pan et al. (2018)		
Maoxian, China	Mountain and shrubbery	1826 (31.70°N, 103.90°E)	Sep 2015 – Aug 2016	offline	3.7	Pan et al. (2018)		
Wuwei, China	Rural	1503 (102.60°N,38.07°E)	Jun 2015	offline	26.5	Xu et al. (2019)		
Bayingbuluke, China	Grassland	2470 (83.71°N, 42.88°E)	Jun 2011	offline	4.0	Xu et al. (2019)		
Louisville, USA	Suburban	1698 (39.99°N, 105.15°W)	Jun – Aug 2011	offline	4.8	Li et al. (2017)		
Greeley, USA	Suburban-agricultural	1492 (40.39°N, 104.75°W)	May – Sep 2015	offline	16.7	Li et al. (2017)		
Kersey, USA	Rural-agricultural	1403 (40.28°N, 104.53°W)	May – Sep 2015	offline	79.4	Li et al. (2017)		
Rocky Mountain National Park, USA	Mountain and forest	2784 (40.28°N, 105.55°W)	Jul – Aug 2006	offline	0.6	Benedict et al. (2013)		
Beaver Meadows, USA	/	2509 (40.36°N, 105.58°W)	Jul – Aug 2006	offline	0.7	Benedict et al. (2013)		
Timber Creek, USA	/	2767 (40.38°N, 105.85°W)	Jul – Aug 2006	offline	0.3	Benedict et al. (2013)		
Gore Pass, USA	/	2641 (40.12°N, 106.53°W)	Jul – Aug 2006	offline	0.4	Benedict et al. (2013)		
Happo, Japan	Mountain and forest	1850 (36.69°N, 137.80°W)	2003 – 2012	offline	0.4	Ban et al. (2016)		

Table S3 Statistical parameters of WTM, SDZ and BMS.

Site	DTW	Euclidean distance	r	RMSD	MAB
WTM and SDZ	725.2	81.9	0.74	4.5	3.0
WTM and BMS	2140.7	265.2	0.67	15.7	11.7

The causality influence of individual meteorological factors on NH₃ concentration.

By applying the CCM method to two time-series variables, their coupling could be understood based on an output convergent map. If the interaction between two variables is featured using generally convergent curves with increasing time series length, then the causality is detected. On the contrary, if the interaction between the two variables is featured as curves without any general trend, then there is no causality between the two variables. The predictive skills ρ -value is a direct indicator of quantitative causality, ranging from 0 to 1, and presents the strength of the impacts from one variable on another variable.

In the CCM algorithm, the parameter E (embedding dimension) of different meteorological factors in this study was adopted at different values depending on the relations of embedding dimension and ρ -value. The E value that could indicate the dynamics of data unfolded best was selected. τ (time lag) was set to 1 to create a shadow manifold. Our result was iterated 100 times to get an optimum result and then tested for the significance of the causal signal. If ρ is convergent to a certain value (in other words, $\Delta \rho$ is approaching 0) with increasing time series, then the causality is detected and the ultimate ρ value for the coupling is set as the convergent constant.

As Fig. 3 demonstrates, the coupling between meteorological factors and NH₃ concentration can be bidirectional. However, we just focus on the direction of influence from meteorological parameters to NH₃ concentration in this study.

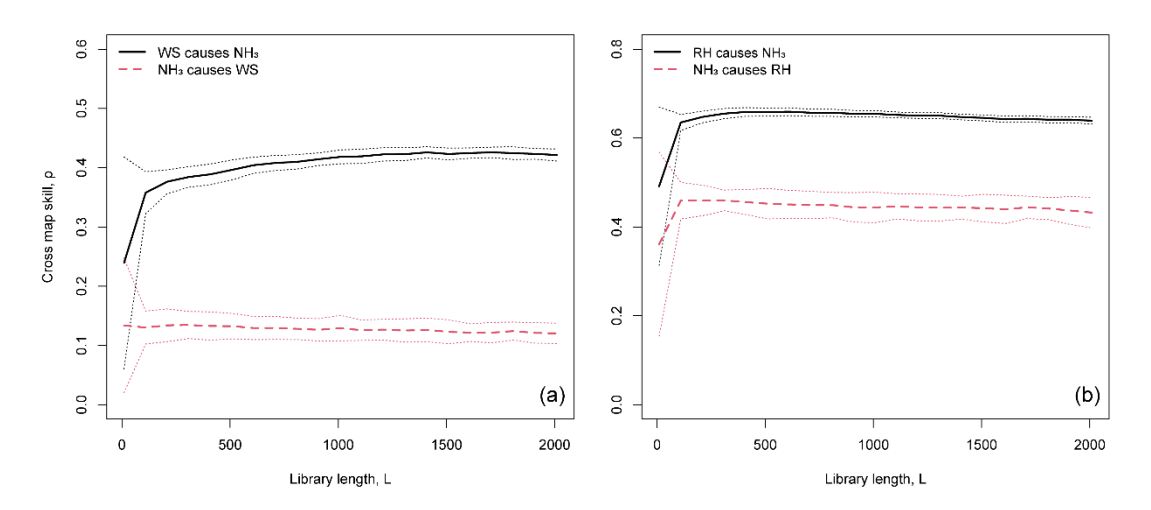


Fig.S2. Convergence cross mapping plot sample, showing the variation of bidirectional predictive skill value (ρ) and length of data time series (L) (a) NH₃ vs WS, (b) NH₃ vs RH. The dot lines represent \pm 1 standard errors.

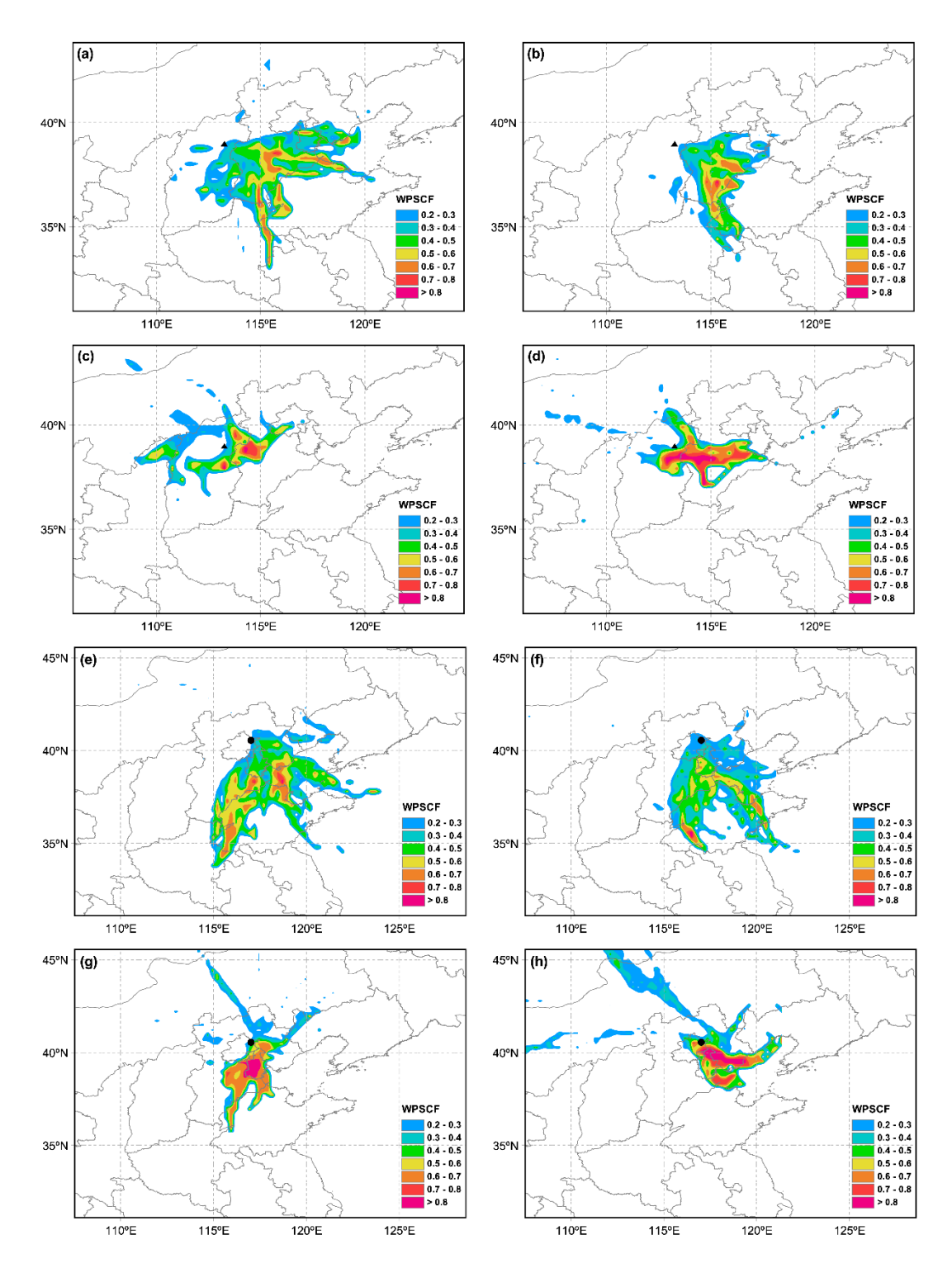


Fig. S3. Potential source contribution analysis of NH_3 in different seasons. (a), (b), (c), and (d) are the PSCF maps of WTM in four seasons, respectively. (e), (f), (g), and (h) are the results of SDZ in four seasons, respectively.

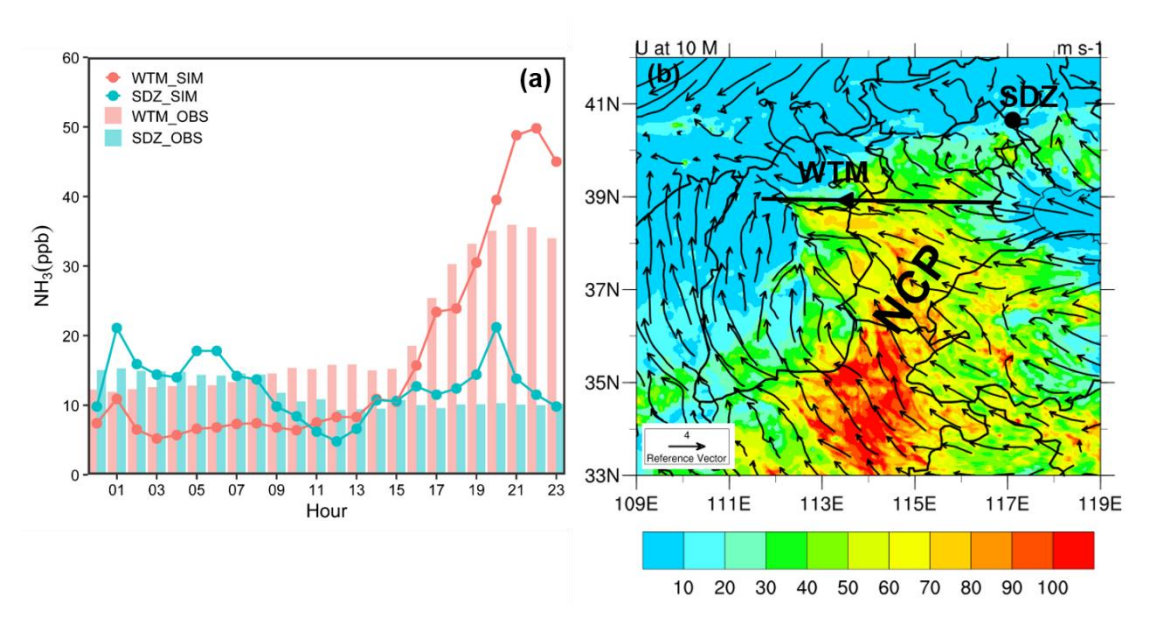


Fig. S4. Diurnal variation of observed and simulated NH₃ concentration (a) and spatial distribution of simulated concentration of NH₃ (unit: ppb) and wind vectors at the surface layer at 19:00 May 12, 2021 (b). The black solid lines represent the locations of the selected vertical cross sections discussed below. The black triangle and dot indicate the location of WTM and SDZ siteS, respectively.

References:

Ban, S., Matsuda, K., Sato, K., and Ohizumi, T.: Long-term assessment of nitrogen deposition at remote EANET sites in Japan, Atmospheric Environment, 146, 70-78, https://doi.org/10.1016/j.atmosenv.2016.04.015, 2016.

Benedict, K. B., Day, D., Schwandner, F. M., Kreidenweis, S. M., Schichtel, B., Malm, W. C., and Collett, J. L.: Observations of atmospheric reactive nitrogen species in Rocky Mountain National Park and across northern Colorado, Atmospheric Environment, 64, 66-76, https://doi.org/10.1016/j.atmosenv.2012.08.066, 2013.

Li, Y., Thompson, T. M., Van Damme, M., Chen, X., Benedict, K. B., Shao, Y., Day, D., Boris, A., Sullivan, A. P., Ham, J. J. A. C., and Physics: Temporal and spatial variability of ammonia in urban and agricultural regions of northern Colorado, United States, 17, 1-50, 2017.

Pan, Y., Tian, S., Zhao, Y., Zhang, L., Zhu, X., Gao, J., Huang, W., Zhou, Y., Song, Y., Zhang, Q., and Wang, Y.: Identifying Ammonia Hotspots in China Using a National Observation Network, Environmental Science & Technology, 52, 3926-3934, 10.1021/acs.est.7b05235, 2018.

Xu, W., Zhang, L., and Liu, X.: A database of atmospheric nitrogen concentration and deposition from the nationwide monitoring network in China, Scientific Data, 6, 51, 10.1038/s41597-019-0061-2, 2019.